





ORIGINAL ARTICLE

Diabetes induced by checkpoint inhibition in nonobese diabetic mice can be prevented or reversed by a JAK1/JAK2 inhibitor

Tingting Ge^{1,2}, Amber-Lee Phung³, Gaurang Jhala¹, Prerak Trivedi¹, Nicola Principe³, David J De George^{1,2}, Evan G Pappas¹, Sara Litwak¹, Laura Sanz-Villanueva^{1,2} , Tara Catterall¹, Stacey Fynch¹, Louis Boon⁴, Thomas W Kay^{1,2} , Jonathan Chee³ , Balasubramanian Krishnamurthy^{1,2} & Helen E Thomas^{1,2} 

¹Immunology and Diabetes Unit, St Vincent's Institute, Fitzroy, VIC, Australia

²The University of Melbourne, Parkville, VIC, Australia

³National Centre for Asbestos Related Diseases, Institute for Respiratory Health, The University of Western Australia, Crawley, WA, Australia

⁴JJP Biologics, Warsaw, Poland

Correspondence

HE Thomas, Immunology and Diabetes Unit,
St Vincent's Institute, Fitzroy,
VIC 3065, Australia.
E-mail: hthomas@svi.edu.au

Received 25 April 2022;

Revised 16 August and 5 October 2022;

Accepted 7 October 2022

doi: 10.1002/cti2.1425

Clinical & Translational Immunology
2022; 11: e1425

Abstract

Objectives. Immune checkpoint inhibitors have achieved clinical success in cancer treatment, but this treatment causes immune-related adverse events, including type 1 diabetes (T1D). Our aim was to test whether a JAK1/JAK2 inhibitor, effective at treating spontaneous autoimmune diabetes in nonobese diabetic (NOD) mice, can prevent diabetes secondary to PD-L1 blockade. **Methods.** Anti-PD-L1 antibody was injected into NOD mice to induce diabetes, and JAK1/JAK2 inhibitor LN3103801 was administered by oral gavage to prevent diabetes. Flow cytometry was used to study T cells and beta cells. Mesothelioma cells were inoculated into BALB/c mice to induce a transplantable tumour model. **Results.** Anti-PD-L1-induced diabetes was associated with increased immune cell infiltration in the islets and upregulated MHC class I on islet cells. Anti-PD-L1 administration significantly increased islet T cell proliferation and islet-specific CD8⁺ T cell numbers in peripheral lymphoid organs. JAK1/JAK2 inhibitor treatment blocked IFN γ -mediated MHC class I upregulation on beta cells and T cell proliferation mediated by cytokines that use the common γ chain receptor. As a result, anti-PD-L1-induced diabetes was prevented by JAK1/JAK2 inhibitor administered before or after checkpoint inhibitor therapy. Diabetes was also reversed when the JAK1/JAK2 inhibitor was administered after the onset of anti-PD-L1-induced hyperglycaemia. Furthermore, JAK1/JAK2 inhibitor intervention after checkpoint inhibitors did not reverse or abrogate the antitumour effects in a transplantable tumour model. **Conclusion.** A JAK1/JAK2 inhibitor can prevent and reverse anti-PD-L1-induced diabetes by blocking IFN γ and γ C cytokine activities. Our study provides preclinical validation of JAK1/JAK2 inhibitor use in checkpoint inhibitor-induced diabetes.

Keywords: cytokines, CD8⁺ T cells, immune checkpoint inhibitor-induced diabetes, JAK inhibitor, NOD mice

INTRODUCTION

Immune checkpoint signalling pathways are important tolerance mechanisms that protect the host from inappropriate immune responses and excessive inflammation.¹ PD-1 is an inhibitory checkpoint molecule upregulated on activated T cells.² Upon binding to its ligands, PD-L1 or PD-L2, on antigen-presenting cells (APCs), tumour or tissue cells, the PD-1/PD-L1 signalling pathway can drive cell apoptosis, negatively regulating T cell activation and proliferation.^{3,4}

Tumours exploit inhibitory immune checkpoints such as PD-L1 to escape immune attack. Antibodies that block the PD-1/PD-L1 interaction, termed immune checkpoint inhibitors, remove the negative regulation tumours impose on T cell function and are now approved as treatment for multiple cancers.^{5–7} However, as checkpoint inhibitors remove the negative regulation on the immune system, they can cause toxicities known as immune-related adverse events.^{8,9} Immune-related adverse events occur in multiple systems, including skin, gastrointestinal tract, liver and the endocrine system, and present similarly to autoimmune diseases. These immune-related adverse events can be improved in many cases using corticosteroids and immune modulators. However, immune-related endocrine toxicities including hypophysitis, thyroid dysfunction, type 1 diabetes (T1D) and adrenal insufficiency¹⁰ are irreversible; in many cases, this is because the endocrine cells have been destroyed.^{9,11} Checkpoint inhibitor-induced diabetes is rare (0.2–1.0%), but when it occurs it is often a life-threatening metabolic emergency.^{12–15}

In nonobese diabetic (NOD) mice, genetic deficiency in either PD-1 or PD-L1 accelerates diabetes onset, which is associated with enhanced T cell proliferation and increased ratio of CD8⁺ to CD4⁺ T cell numbers.^{16–18}

Spontaneous diabetes is characterised by the proliferation of autoreactive T cells and MHC class I upregulation on beta cells, which are mediated by common gamma chain (γ C) cytokines and IFN- γ , respectively.^{19–23} In this study, our first aim was to investigate whether these hallmarks of spontaneous diabetes also occur in checkpoint inhibitor-induced diabetes.

Both γ C cytokines and IFN- γ function through the Janus kinase (JAK)-signal transducer and activator of transcription (STAT) pathway. In a previous study, we showed that JAK inhibitors reduced T cell proliferation by blocking γ C cytokine activity and inhibited MHC class I upregulation on beta cells by blocking IFN- γ .²³ As a result, spontaneous diabetes was reversed in NOD mice by blocking cytokine effects on both beta cells and T cells.^{23,24} The aim of the current study was to investigate the mechanisms of checkpoint inhibitor-induced diabetes and to test whether a JAK1/JAK2 inhibitor has activity in diabetes secondary to PD-L1 blockade.

RESULTS

Anti-PD-L1 increases immune cell infiltration in islets and accelerates diabetes

To investigate the effects of anti-PD-L1 on diabetes onset, we injected 7–8-week-old female NOD mice with anti-PD-L1 antibody and evaluated the immune cell infiltration in NOD mice. This resulted in rapid diabetes development (Figure 1a). 72.7% (8/11) of the mice developed diabetes within 2 weeks of starting anti-PD-L1 treatment with diabetes beginning at day 9. The proportion of CD45⁺ immune cells and MHC class I expression were measured by flow cytometry (Supplementary figure 1a). Anti-PD-L1 treatment significantly upregulated MHC class I expression on islet beta cells in NOD mice (Figure 1b, c). The proportion of CD45⁺ cells in islets was significantly increased in anti-PD-L1-treated mice compared with PBS-treated control mice (Figure 1d, e). These data confirm that antibody blockade of PD-L1 accelerated diabetes onset in NOD mice, which was associated with increased immune cell infiltration into islets, and MHC class I upregulation on beta cells.

Anti-PD-L1 increases islet T cell proliferation and the number of IGRP_{206–214}-specific CD8⁺ T cells in peripheral lymphoid organs

We investigated the effects of anti-PD-L1 treatment on T cells because they are the main

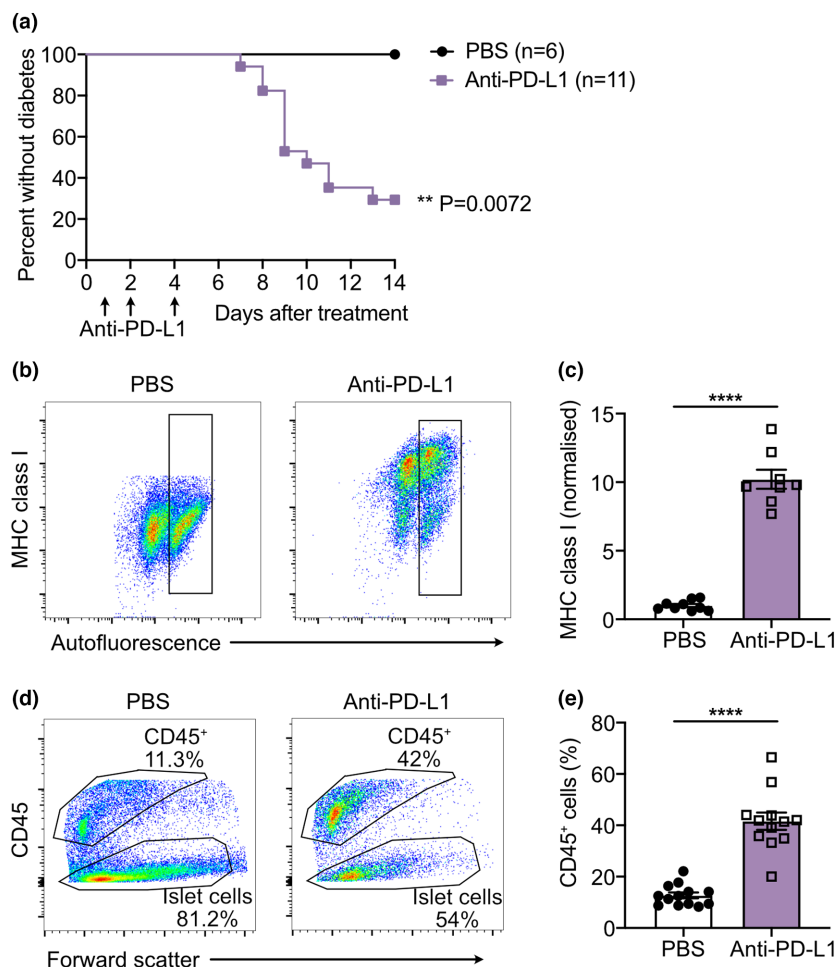


Figure 1. Anti-PD-L1 increases beta cell MHC class I expression and immune cell infiltration in islets. **(a)** Diabetes incidence of 7-week-old female NOD mice treated with anti-PD-L1 antibody on days 1, 3 and 5, indicated with arrows, $**P = 0.0072$, log-rank (Mantel-Cox) test. **(b)** Representative dot plots of MHC class I (H-2Kd) expression. Beta cells are identified by autofluorescence (boxed area). **(c)** Pooled data of normalised mean fluorescence intensity (MFI) of MHC class I on islet cells measured by flow cytometry in 7-week-old female NOD mice treated with PBS and anti-PD-L1. The MFI of MHC class I in anti-PD-L1-treated mice was divided by the average MFI of MHC class I in PBS-treated mice to get the fold change in each independent experiment. **(d)** Representative flow cytometry plots showing gating of immune cells ($CD45^+$) and islet cells with the percentage of live cells shown. **(e)** Pooled data of the proportion of $CD45^+$ cells in islets from 7-week-old female NOD mice treated with PBS ($N = 14$) and anti-PD-L1 ($N = 12$), from two independent experiments. Data show individual mice with mean \pm SEM, $****P < 0.0001$, Student's t -test.

mediators of spontaneous diabetes in NOD mice. The number of $CD4^+$ and $CD8^+$ T cells increased in islets after anti-PD-L1 treatment (Figure 2a, b). T cell proliferation was measured by *in vivo* BrdU incorporation (Supplementary figure 1b). The percentage of $CD8^+BrdU^+$ T cells in islets of anti-PD-L1-treated mice was significantly higher than that in PBS-treated mice (Figure 2c, d). Proliferation of $CD4^+$ T cells in the islets was also increased after anti-PD-L1 treatment (Figure 2e, f) but to a lesser extent than for $CD8^+$ T cells. $CD8^+$ T cells recognising IGRP_{206–214} are the most

prevalent diabetogenic $CD8^+$ T cells in NOD mice.²⁸ IGRP_{206–214}-specific $CD8^+$ T cells were quantified in both peripheral lymphoid organs (PLO, consisting of pooled spleen and non-draining lymph nodes) and pancreatic lymph node (PLN) using tetramer enrichment and flow cytometry (Supplementary figure 1c). The number of IGRP_{206–214}-specific $CD8^+$ T cells in PLO (Figure 2g, h) and PLN (Figure 2i, j) was increased after anti-PD-L1 treatment, especially in the 8/15 mice that were diabetic when analysed.

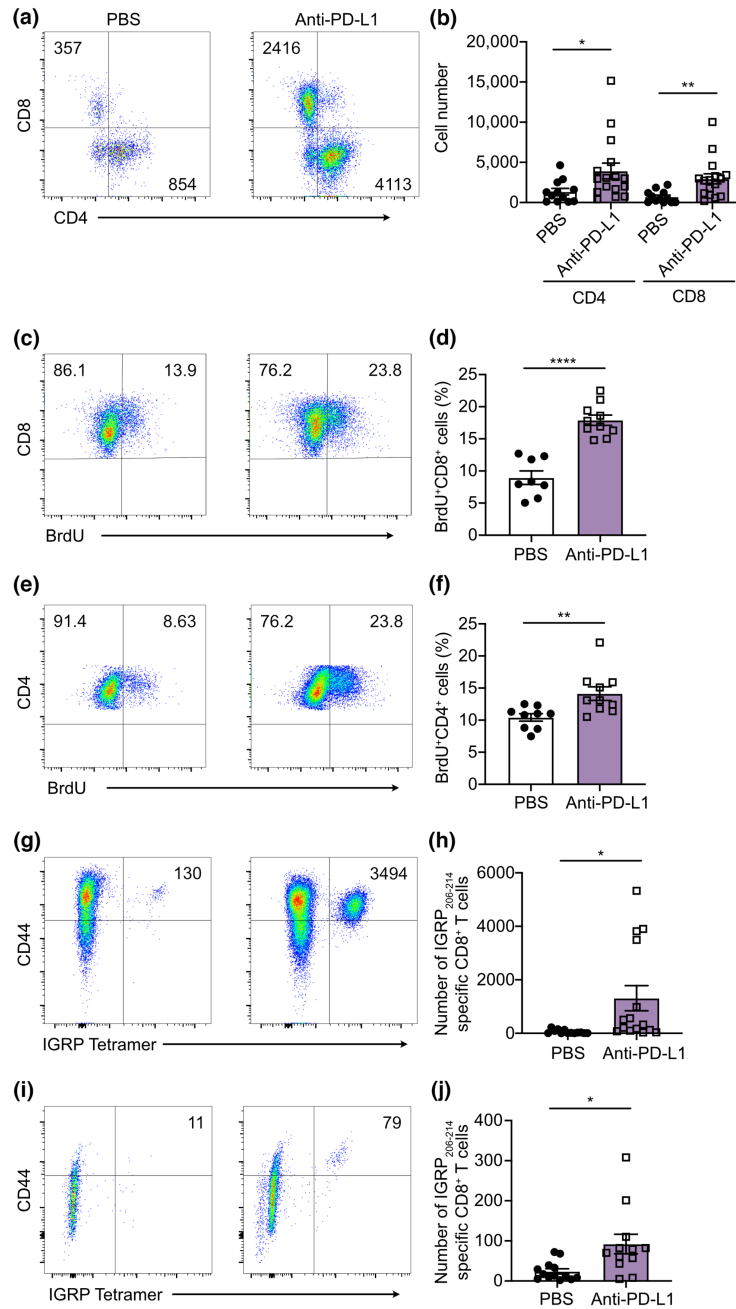


Figure 2. Anti-PD-L1 increases islet CD8⁺ T cell proliferation and the number of IGRP₂₀₆₋₂₁₄-specific CD8⁺ T cells in peripheral lymphoid organs. **(a)** Representative flow cytometry plots of CD4 and CD8 staining in islet T cells showing the number of cells in each gate. **(b)** Pooled data showing the number of CD4⁺ T cells and CD8⁺ T cells from the islets of 7-week-old female NOD mice treated with PBS (N = 12) or anti-PD-L1 (N = 16), combined from four independent experiments. Data show individual mice with mean ± SEM, P-values are only provided when significant: *P = 0.0406, **P = 0.0061, Student's t-test. **(c, e)** Representative flow cytometry plots of BrdU in CD8⁺ T cells **(c)** and CD4⁺ T cells **(e)** showing the percentage of cells in each quadrant. **(d, f)** Pooled data showing the proportion of BrdU-positive CD8⁺ **(d)** and CD4⁺ **(f)** T cells from the islets of 7-week-old female NOD mice treated with PBS (N = 9) or anti-PD-L1 (N = 10), combined from three independent experiments. Data show individual mice with mean ± SEM. P-values are only provided when significant: **P = 0.0086, ****P < 0.0001, Student's t-test. **(g, i)** Representative plots of IGRP₂₀₆₋₂₁₄ tetramer staining in the pooled spleen and peripheral lymph nodes **(g)** and pancreatic lymph node **(i)** showing the number of tetramer⁺CD44⁺ cells. **(h, j)** Pooled data showing the absolute numbers of IGRP₂₀₆₋₂₁₄-specific CD8⁺ T cells in the pooled spleen and peripheral lymph nodes **(h)** and pancreatic lymph node **(j)** from PBS (N = 13) or anti-PD-L1 (N = 15) treatment, combined from four independent experiments. Data show individual mice with mean ± SEM. P-values are only provided when significant: *P = 0.0198 **(h)**, *P = 0.0103 **(j)**, Student's t-test.

In summary, we have confirmed that the PD-L1/PD-1 interaction has a profound effect on controlling autoimmune diabetes in genetically susceptible mice. PD-L1 blockade resulted in acute diabetes and increased immune infiltration into the islets, with MHC class I upregulation on beta cells, enhanced proliferation of T cells and increased numbers of islet-specific CD8⁺ T cells, all similar to hallmarks of spontaneous autoimmune diabetes as shown by us and others.^{17,23,25}

A JAK1/JAK2 inhibitor prevents MHC class I expression on islets and reduces insulinitis secondary to anti-PD-L1 treatment

We evaluated the effect of the JAK1/JAK2 inhibitor LN3103801 in combination with anti-PD-L1 treatment. JAK1/JAK2 inhibitor administered prior to anti-PD-L1 injection prevented MHC class I upregulation on beta cells (Figure 3a, b) and prevented the infiltration of CD45⁺ immune cells into islets (Figure 3c, d). It was previously shown that anti-PD1 treatment resulted in an increase in the number of migratory macrophages in islets of NOD mice.¹⁷ We saw a similar increase in the proportion of Ly6C⁺F4/80⁺ monocyte-derived macrophages after anti-PD-L1 treatment, and JAK1/JAK2 inhibitor treatment blocked this increase (Figure 3e, g). There was no change in the proportion of dendritic cells or resident macrophages after anti-PD-L1 or JAK1/JAK2 inhibitor treatment (Figure 3e, f, h). Histologically, 80% of islets in mice treated with anti-PD-L1 and vehicle had extensive immune cell infiltration and beta cell destruction. By contrast, the combination of anti-PD-L1 with prior JAK1/JAK2 inhibitor resulted in significantly reduced insulinitis (Figure 3i, j).

JAK1/JAK2 inhibitor reduces islet T cell proliferation and the number of IGRP_{206–214}-specific CD8⁺ T cells in peripheral lymphoid organs

JAK1/JAK2 inhibitor treatment prevented the increase in number of both CD4⁺ and CD8⁺ T cells in the islets (Figure 4a, b). While the number of T cells was reduced after JAK1/JAK2 inhibitor treatment, the percentage of Foxp3⁺CD4⁺ Treg cells was not changed (Figure 4c, d). T cell proliferation was reduced, consistent with the changes in T cell numbers. The JAK1/JAK2 inhibitor significantly prevented CD4⁺ (Figure 4e, f)

and CD8⁺ (Figure 4g, h) T cell proliferation in the islets. JAK1/JAK2 inhibitor treatment reduced the number of IGRP_{206–214}-specific CD8⁺ T cells in the PLO (Figure 4i, j) and the PLN (Figure 4k, l) after anti-PD-L1 treatment compared with vehicle treatment.

Therefore, JAK1/JAK2 inhibitor treatment can prevent the hallmarks of diabetes development including beta cell MHC class I expression, T cell proliferation and infiltration of immune cells into islets.

JAK1/JAK2 inhibitor prevents or reverses diabetes secondary to anti-PD-L1 treatment

To test whether the JAK1/JAK2 inhibitor can prevent diabetes induced by anti-PD-L1, daily JAK1/JAK2 inhibitor treatment started 4 days before anti-PD-L1 and was maintained for 18 consecutive days. Vehicle-treated mice developed diabetes rapidly after anti-PD-L1 treatment, with 83.3% (5/6) of mice developing diabetes in 2 weeks. However, all JAK1/JAK2 inhibitor-treated mice were free of diabetes during the treatment period. Even 2 weeks after JAK1/JAK2 inhibitor treatment stopped, 66.7% (4/6) of mice remained nondiabetic (Figure 5a). Therefore, JAK1/JAK2 inhibitor treatment can prevent diabetes when it is given prior to anti-PD-L1 treatment. Similar results were seen when we used anti-PD-1 to induce diabetes (Figure 5b).

We next tested whether JAK1/JAK2 inhibitor prevented diabetes development when it was started after completion of anti-PD-L1 treatment. 87.5% (7/8) of mice became diabetic in vehicle-treated mice, but 75% (6/8) of JAK1/JAK2 inhibitor-treated mice were free of diabetes during the treatment time and another 2 weeks after stopping the drug (Figure 5c).

As diabetes secondary to immune checkpoint therapy cannot be predicted in patients, it is more clinically relevant to test whether the JAK1/JAK2 inhibitor can reverse diabetes after it develops. 7–8-week-old female NOD mice were injected with anti-PD-L1 and then monitored for diabetes. JAK1/JAK2 inhibitor or vehicle treatment was started on the day of diabetes diagnosis and continued for 2 weeks. All vehicle-treated mice remained hyperglycaemic (Figure 5d, e), but hyperglycaemia was reversed in 55.6% (5/9) of JAK1/JAK2 inhibitor-treated mice that maintained normal blood glucose levels even after stopping the drug. This suggests that JAK1/JAK2 inhibitor

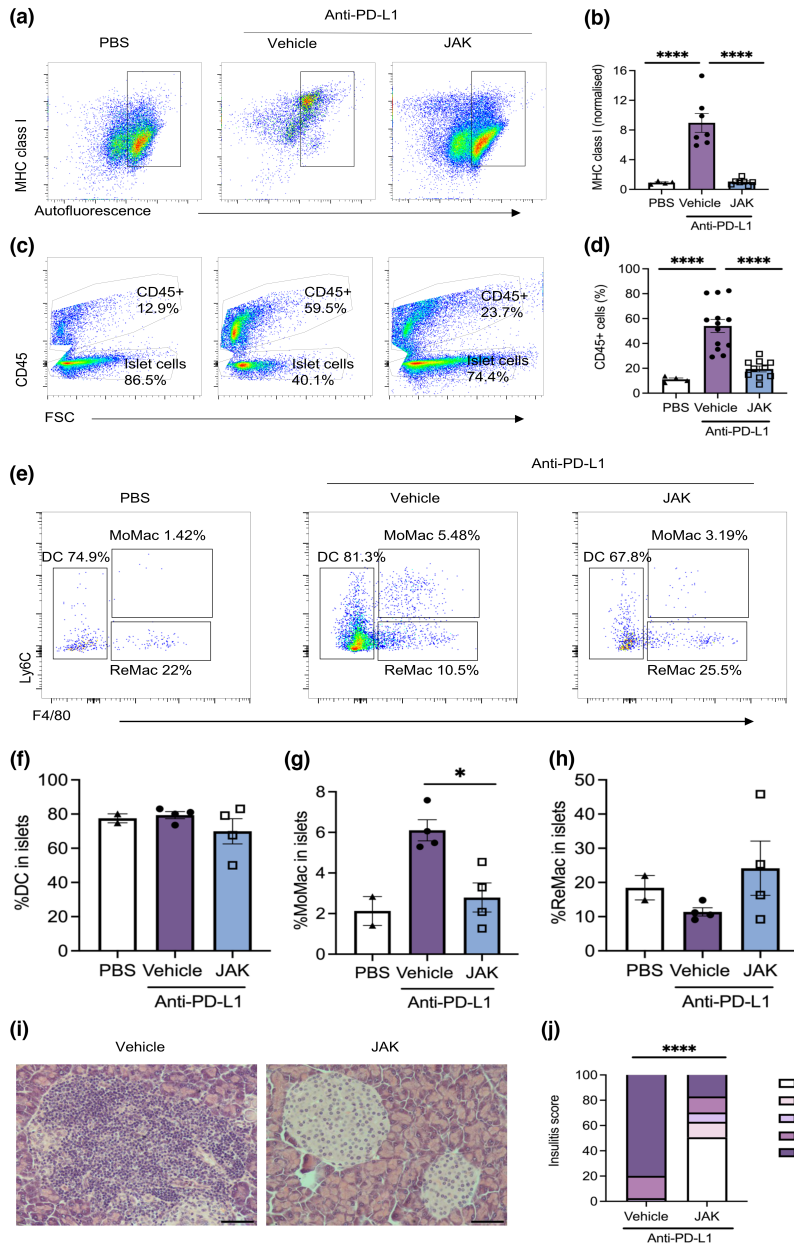


Figure 3. JAK1/JAK2 inhibitor prevents upregulation of MHC class I expression on islets and insulinitis caused by anti-PD-L1. **(a)** Representative plots of islet MHC class I expression measured by flow cytometry. Beta cells (boxed area) are identified by high autofluorescence. **(b)** Pooled data of normalised MFI of MHC class I on beta cells from 7-week-old female NOD mice treated with PBS ($N = 4$) or anti-PD-L1 and vehicle ($N = 7$) or anti-PD-L1 and JAK1/JAK2 inhibitor ($N = 7$), combined from two independent experiments. The MFI of MHC class I in anti-PD-L1-treated mice was divided by the average MFI of MHC class I in PBS mice to get the fold change in each independent experiment. Data show individual mice with mean \pm SEM, **** $P < 0.0001$, one-way ANOVA. **(c)** Representative flow cytometry plots showing the percentage of live CD45⁺ cells and islet cells in islets. **(d)** Pooled data of the percentage of CD45⁺ cells in islets from 7-week-old female NOD mice treated with PBS ($N = 14$) or anti-PD-L1 and vehicle ($N = 13$) or anti-PD-L1 and JAK1/JAK2 inhibitor ($N = 10$), combined from four independent experiments. Data show individual mice with mean \pm SEM, **** $P < 0.0001$, one-way ANOVA. **(e)** Representative plots showing gating for islet dendritic cells (DC), monocyter-derived inflammatory macrophages (MoMac) and resident macrophages (ReMac). **(f–h)** Pooled data showing percentages of **(f)** DC, **(g)** MoMac and **(h)** ReMac cells from islets of 10-week-old female NOD mice treated with PBS ($N = 2$), anti-PD-L1 and vehicle ($N = 4$) or anti-PD-L1 and JAK1/JAK2 inhibitor ($N = 4$). Data show individual mice with mean \pm SEM. * $P < 0.0001$, one-way ANOVA. **(i)** Representative H&E stained sections of pancreas harvested from 7–8-week-old female NOD mice treated with anti-PD-L1 and vehicle or anti-PD-L1 and JAK1/JAK2 inhibitor, magnification 400 \times , scale bar 50 μ m. **(j)** Pooled insulinitis scores, calculated as described in the methods. Data show the pooled scores of 3 levels of the pancreas from $N = 4$ mice/group, **** $P < 0.0001$, two-way ANOVA.

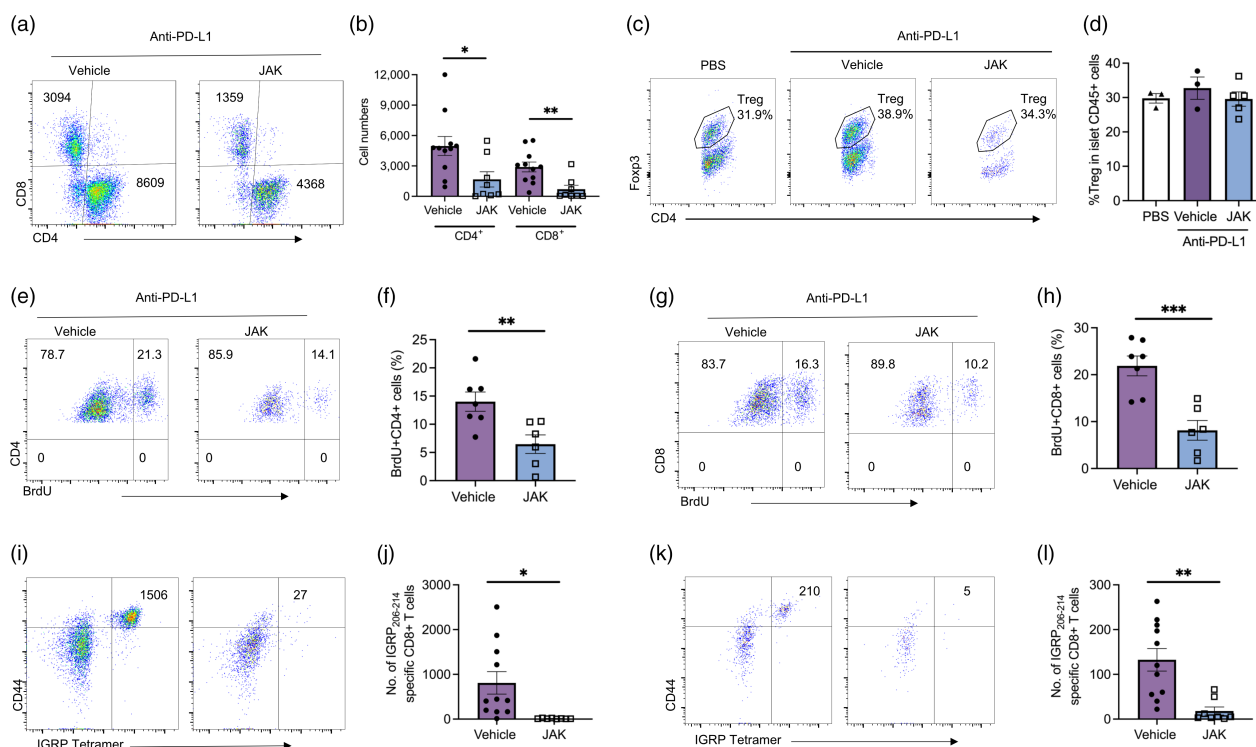


Figure 4. JAK1/JAK2 inhibitor prevents T cell proliferation and reduces the number of IGRP_{206–214}-specific CD8⁺ T cells in peripheral lymphoid organs. **(a)** Representative plots showing the number of CD4⁺ and CD8⁺ T cells in islets measured by flow cytometry. **(b)** Pooled data showing numbers of CD8⁺ and CD4⁺ T cells from 7–8-week-old female NOD mice treated with anti-PD-L1 and vehicle ($N = 11$) or anti-PD-L1 and JAK1/JAK2 inhibitor ($N = 8$), from three independent experiments. Data show individual mice with mean \pm SEM. P -values are only provided when significant: $*P = 0.0190$, $**P = 0.0041$, Student's t -test. **(c)** Representative plots showing Fcpx3 and CD4 staining on islet CD4⁺ T cells. **(d)** Pooled data showing the percentage Fcpx3⁺CD4⁺ islet cells from 10-week-old female NOD mice treated with PBS ($N = 3$), anti-PD-L1 and vehicle ($N = 3$) or anti-PD-L1 and JAK1/JAK2 inhibitor ($N = 5$) from two independent experiments. Data show individual mice with mean \pm SEM. No significant difference was noted between the groups, one-way ANOVA. **(e, g)** Representative flow cytometry plots of BrdU staining in CD4⁺ **(e)** and CD8⁺ **(g)** T cells showing the percentage of cells in each quadrant. **(f, h)** Pooled data showing the proportion of BrdU-positive CD4⁺ **(f)** and CD8⁺ **(h)** T cells from 7-week-old female NOD mice treated with anti-PD-L1 and vehicle ($N = 7$) or anti-PD-L1 and JAK1/JAK2 inhibitor ($N = 6$), from two independent experiments. Data show individual mice with mean \pm SEM. P -values are only provided when significant: $**P = 0.0092$, $***P = 0.0008$, Student's t -test. **(i, k)** Representative plots of IGRP_{206–214} tetramer staining in the pooled spleen and peripheral lymph nodes **(i)** and pancreatic lymph nodes **(k)** showing the number of tetramer⁺CD44⁺ cells. **(j)** and **(l)** Pooled data showing absolute numbers of IGRP_{206–214}-specific CD8⁺ T cells in the pooled spleen and peripheral lymph nodes **(j)** and pancreatic lymph nodes **(l)** from 7-week-old female mice treated with anti-PD-L1 and vehicle ($N = 11$) or anti-PD-L1 and JAK1/JAK2 inhibitor ($N = 8$), from three independent experiments. Data show individual mice with mean \pm SEM. P -values are only provided when significant: $*P = 0.0158$, $**P = 0.0017$, Student's t -test.

treatment can reverse diabetes secondary to PD-L1 blockade and can provide ongoing protection after stopping the drug.

Immune checkpoint inhibitor therapy is repeatedly administered in the clinic. We therefore tested whether the JAK1/JAK2 inhibitor protected mice from diabetes when they were given a second round of anti-PD-L1 treatment (Figure 5f). NOD mice were treated with anti-PD-L1 followed by JAK inhibitor or vehicle for 2 weeks. All the vehicle-treated mice (3/3) and four of the JAK inhibitor-treated mice (4/15) became diabetic. After 3 days with no therapy,

the nondiabetic mice that had previously been given JAK inhibitor were again treated with anti-PD-L1 and then divided into two groups receiving treatment with JAK1/JAK2 inhibitor or vehicle for a further 2 weeks. None of the JAK inhibitor-treated (0/7) and one of the vehicle-treated mice (1/8) became diabetic (Figure 5f). The islets from these mice still had a low proportion of CD45⁺ cells (Figure 5g, h) and MHC class I expression (Figure 5i, j) when compared to untreated NOD mice of a similar age, even 3 weeks after stopping JAK1/JAK2 inhibitor treatment. These data indicate that the 2 weeks of JAK

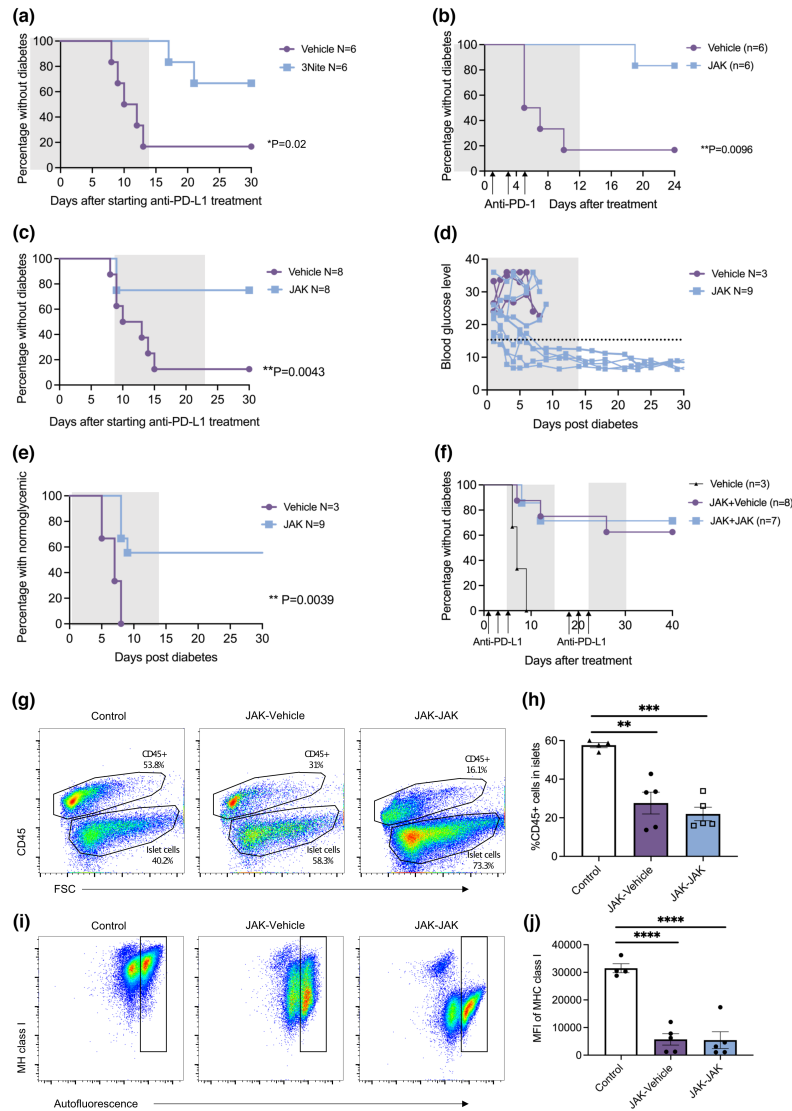


Figure 5. JAK1/JAK2 inhibitor prevents or reverses diabetes secondary to anti-PD-L1 treatment. **(a)** 7–8-week-old female NOD mice were treated with vehicle (*N* = 6) or JAK1/JAK2 inhibitor (*N* = 6) for 4 days before anti-PD-L1 treatment (day 1, 3 and 5 indicated with arrows) and continuing until day 14 after anti-PD-L1 treatment (shaded area). Survival curve analysis of the NOD mice is shown, from one experiment, **P* = 0.02, log-rank (Mantel-Cox) test. **(b)** 9-week-old female NOD mice were treated with vehicle (*N* = 6) or JAK1/JAK2 inhibitor (*N* = 6) for 4 days before anti-PD1 (day 1, 3 and 5 indicated with arrows) and continuing until day 12 after anti-PD-L1 treatment (shaded area). Survival curve analysis is shown, from one experiment. ***P* = 0.0096, log-rank (Mantel-Cox) test. **(c)** 7–8-week-old female NOD mice were treated with anti-PD-L1 at day 1, 3 and 5 as indicated with arrows and then started on vehicle (*N* = 8) or JAK1/JAK2 inhibitor (*N* = 8) at day 5 for 14 days (shaded area). Survival curve analysis of the NOD mice is shown, from two independent experiments, **P* = 0.0043, log-rank (Mantel-Cox) test. **(d, e)** Blood glucose levels were monitored in 7–8-week-old female NOD mice after anti-PD-L1 treatment. Diabetic mice (with blood glucose > 15 mmol L⁻¹) were then treated with JAK1/JAK2 inhibitor (*N* = 9) or vehicle (*N* = 3) for 14 days (shaded area). Blood glucose levels of individual mice **(d)** and survival curve analysis of the normoglycaemic mice **(e)** is shown, combined from two independent experiments, ***P* = 0.0039, log-rank (Mantel-Cox) test. **(f)** 9-week-old female NOD mice were treated with anti-PD-L1 on day 1, 3 and 5 as indicated with arrows. Mice were then treated with either vehicle (*N* = 3) or JAK1/JAK2 inhibitor (*N* = 15) for 2 weeks starting on day 5 (shaded area). Three days after stopping JAK1/JAK2 inhibitor treatment, the nondiabetic mice (*N* = 11) were treated again with anti-PD-L1 (arrows on days 18, 20 and 22) and randomised to vehicle (JAK + vehicle, *N* = 6) or JAK1/JAK2 inhibitor (JAK + JAK, *N* = 5) treatment starting on day 22 for 8 days (shaded area). Survival curve analysis is shown, with no significant difference noted between JAK + vehicle and JAK + JAK groups, log-rank (Mantel-Cox) test. **(g, i)** Representative flow cytometry plots showing the percentage of live CD45⁺ cells in islets **(g)** and MHC class I expression on beta cells **(i)**. **(h, j)** Pooled data of the percentage of CD45⁺ cells in islets **(h)** and normalised MFI of MHC class I on beta cells **(j)** from untreated 16-week-old female NOD (*N* = 4), JAK + vehicle (*N* = 5) or JAK + JAK (*N* = 5) mice from **f**, harvested 3 weeks after stopping JAK inhibitor treatment. Data show individual mice with mean ± SEM, ***P* < 0.01, ****P* < 0.001, *****P* < 0.0001, one-way ANOVA.

inhibitor treatment provided prolonged protection from immune infiltration and anti-PD-L1-induced diabetes.

JAK1/JAK2 inhibitor after immune checkpoint blockade does not reverse or abrogate the antitumour effects

To assess whether the JAK1/JAK2 inhibitor reduced the efficacy of checkpoint inhibitor therapy-mediated antitumour immunity, we utilised a transplantable tumour model treated with immune checkpoint blockade (ICPB) therapy (anti-CTLA-4+anti-PD-L1).²⁶ We previously established that pre-checkpoint inhibitor STAT1 signalling is crucial for antitumour responses in this model, and we hypothesised that JAK1/JAK2 inhibitor treatment concurrently with checkpoint inhibitors would impede antitumour responses. Concurrent JAK1/JAK2 inhibitor and ICPB treatment significantly increased tumour growth (JAK inhibitor + ICPB vs Vehicle + ICPB, day 17 to 27, $P < 0.05$) (Figure 6a) and reduced overall median survival (JAK inhibitor + ICPB vs. Vehicle + ICPB, 21.5 days vs. 23 days, $P = 0.0081$) (Figure 6b) compared with ICPB alone. 4/10 mice showed tumour regression or growth delay with ICPB alone, with one mouse displaying a durable, long-term tumour regression. However, responses were completely abrogated in combination JAK1/JAK2 inhibitor and ICPB group (0/10 mice) (Supplementary figure 2a–d). This suggested that JAK signalling is crucial for the initiation of checkpoint inhibitor-mediated antitumour responses.

We next assessed whether JAK1/JAK2 inhibitor administered after completion of ICPB treatment would abrogate antitumour responses. JAK1/JAK2 inhibitor treatment after checkpoint inhibitors (Figure 6c) resulted in a small but significant delay in tumour growth compared with JAK1/JAK2 inhibitor monotherapy or vehicle treatment (JAK inhibitor + ICPB vs. JAK inhibitors, day 7 to day 26, $P < 0.05$; JAK inhibitor + ICPB vs Vehicle, day 19 to day 21, $P < 0.05$). Checkpoint inhibitors significantly increased overall survival regardless of JAK1/JAK2 inhibitor treatment (JAK inhibitor + ICPB vs. JAK inhibitor, $P = 0.0091$; ICPB vs. Vehicle, $P = 0.02$) (Figure 6d). Although the effect of ICPB in this model is modest, importantly, overall tumour growth and median survival was similar when JAK1/JAK2 inhibitor after ICPB was compared with ICPB alone (JAK inhibitor + ICPB vs

Vehicle + ICPB, 24 days vs 26 days, $P = 0.6$) (Figure 6d). 3/9 mice treated with ICPB partially responded, demonstrating a delay in tumour growth. A similar number of mice displayed durable responses to ICPB (3/13 in JAK inhibitor + ICPB vs 2/13 in Vehicle + ICPB) (Supplementary figure 2e–h), suggesting that JAK1/JAK2 inhibitor after ICPB completion did not reverse or abrogate the antitumour effects of checkpoint inhibitors in this model.

DISCUSSION

Our study found that anti-PD-L1 accelerated diabetes development in NOD mice was associated with increased MHC class I expression on islet cells and T cell proliferation. The JAK1/JAK2 inhibitor LN3103801 prevented anti-PD-L1 effects on T cells and beta cells, resulting in durable prevention or reversal of anti-PD-L1-induced diabetes. Furthermore, JAK1/JAK2 inhibitor after checkpoint inhibitor therapy did not impair the checkpoint inhibitor-mediated anticancer response.

JAK1/JAK2 inhibitor treatment was able to prevent and reverse checkpoint inhibitor-induced diabetes in NOD mice. 60–85% of checkpoint inhibitor-induced diabetes patients present with life-threatening diabetic ketoacidosis (DKA) because of rapid destruction of beta cells,²⁹ so early intervention or prevention is necessary to decrease the mortality and to improve the prognosis. JAK inhibitors have been approved by the FDA for myelofibrosis, rheumatoid arthritis (RA) and other autoimmune diseases, and clinical data show that JAK inhibitors are safe and well-tolerated in these patients.^{30,31} Recent studies looking at the side effects of JAK inhibitors in comparison with anti-TNF therapeutics in RA will help identify groups of patients at increased risk of side effects including cardiovascular disease or certain cancers such as lung cancer and lymphoma, for example, smokers.³² Few RA patients using JAK inhibitors stop treatment because of infection or changes in immune cell counts, which are usually transient.³³

In our study, we have shown that the JAK1/JAK2 inhibitor LN3103801 reversed new-onset diabetes in NOD mice after anti-PD-L1 treatment. Combined with the safety of JAK inhibitors in clinical use, our study provides strong preclinical evidence to test JAK inhibitors in checkpoint inhibitor-induced diabetes. This is especially true because the need for JAK inhibitor treatment may not be long-lived.

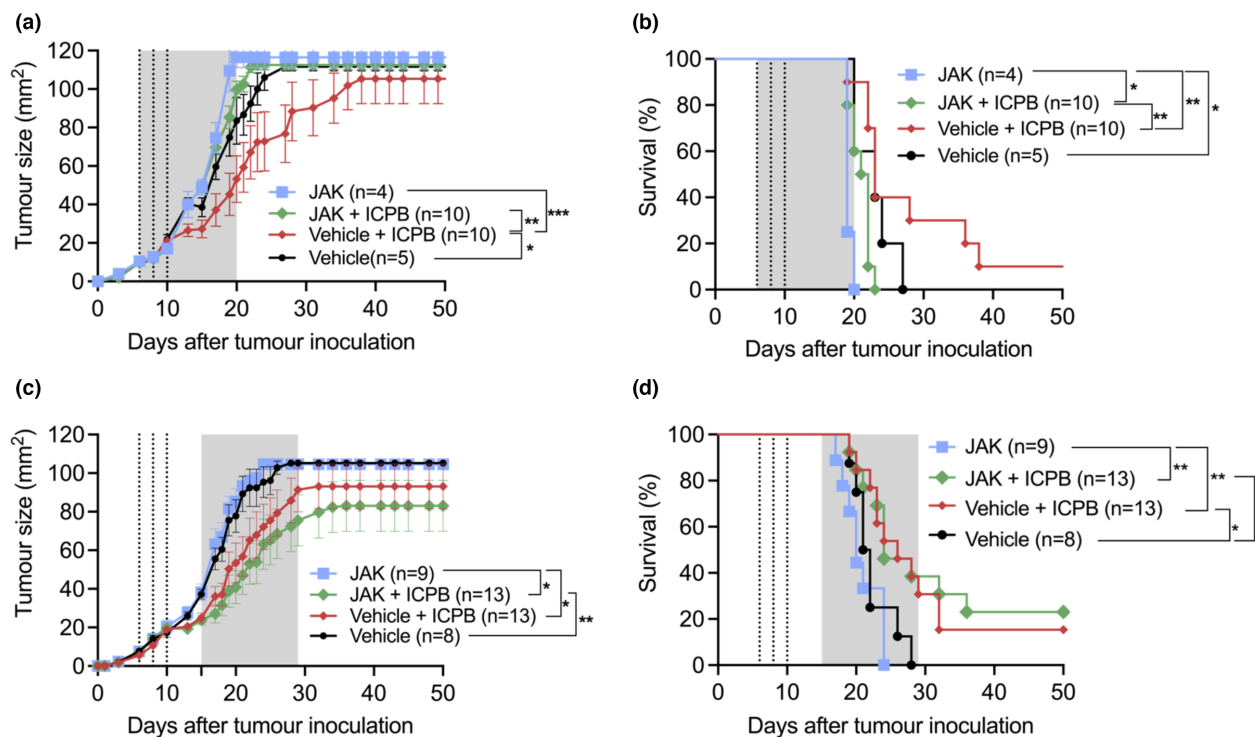


Figure 6. JAK1/JAK2 inhibitor after immune checkpoint inhibitors does not abrogate the antitumour effects. **(a)** BALB/c.J mice were inoculated with mesothelioma cell lines and started with anti-CTLA-4 and anti-PD-L1 (ICPB) on day 6, 8 and 10 (indicated with arrows). JAK1/JAK2 inhibitor or vehicle was administered from day 6 to day 20 (shaded area). Mean tumour growth in JAK inhibitor ($N = 4$), JAK inhibitor + ICPB ($N = 10$), vehicle ($N = 5$) and vehicle + ICPB ($N = 10$). **(b)** Survival curve analysis for data shown in A. $*P < 0.05$, $**P < 0.005$, $***P < 0.001$ and $*P = 0.0158$ for JAK inhibitor vs Vehicle, $*P = 0.0041$ for JAK inhibitor + ICPB vs Vehicle + ICPB, log-rank (Mantel-Cox) test. **(c)** BALB/c.J mice were injected with mesothelioma cell lines and started with ICPB on day 6, 8 and 10 (indicated with arrows). JAK1/JAK2 inhibitor or vehicle treatment was administered from day 15 to day 29 (shaded area). Mean tumour growth in JAK inhibitor ($N = 9$), JAK inhibitor + ICPB ($N = 13$), vehicle ($N = 8$) and vehicle + ICPB ($N = 13$), from two independent experiments. **(d)** Survival curve analysis for data shown in c. $*P < 0.05$, $**P < 0.005$, and no significant difference was noted between JAK inhibitor vs Vehicle or JAK inhibitor + ICPB vs Vehicle + ICPB.

Our data in NOD mice suggest that the enhanced autoimmune responses induced by checkpoint inhibitor therapy may be relatively transient and diabetes does not develop when the drug is ceased. This is unlike the autoimmune response seen at the onset of spontaneous diabetes when it is assumed JAK inhibitor therapy, if effective, would have to be indefinite. The use of JAK inhibitors in relation to subsequent courses of checkpoint inhibitor therapy needs to be further considered and explored.

Mechanistic studies have shown that PD-L1 blockade activates T cells resident in islets or PLNs. Activated T cells then produce cytokines locally and these, including γ c cytokines, such as IL-2, IL-15 and IL-21, regulate T cell expansion and survival.^{34–36} Increased T cell proliferation and an increase in the number of antigen-specific CD8⁺ T cells were seen after anti-PD-L1 treatment. T cells are essential for diabetes since deletion of either

CD4⁺ or CD8⁺ T cells was able to prevent checkpoint inhibitor-induced diabetes in NOD mice.¹⁷ In addition to T cells, other immune cells, including macrophages, might also be involved in checkpoint inhibitor-induced diabetes.¹⁷ In addition, blocking PD-L1 with antibodies partially reduced the expansion of Treg cells,³⁷ which impaired the role of Treg cells to inhibit T cell proliferation and effector function.^{38,39}

Activated T cells produce IFN- γ , which is important for the involvement of beta cells in diabetes development. It is well recognised that IFN- γ is primarily responsible for increased MHC class I expression in type 1 diabetes.²² Direct interaction between MHC class I and TCR is required for diabetes development,⁴⁰ and we observed upregulated MHC class I on islet cells in checkpoint inhibitor-induced diabetes.

Our data show that two hallmarks of spontaneous diabetes, MHC class I upregulation

on beta cells and T cell proliferation, are also seen in anti-PD-L1-induced diabetes.^{22,25,41} JAK1/JAK2 inhibitor treatment prevented checkpoint inhibitor-induced and spontaneous diabetes by blocking the effect of cytokines on both T cells and beta cells⁴⁰ and perhaps other cell types not studied here. T cell proliferation was reduced because the activity of γ c cytokines was blocked, as shown by the reduced number of islet T cells and IGRP_{206–214}-specific CD8⁺ T cells in PLN and PLO. Also, IFN- γ -mediated MHC class I upregulation can be blocked by JAK inhibitors, resulting in low MHC class I expression and weakened interactions between T cells and beta cells.²⁴ In summary, JAK1/JAK2 inhibitor treatment prevented anti-PD-L1-induced diabetes by blocking γ c cytokine activity-mediated T cell proliferation and blocking IFN- γ -induced MHC class I upregulation on beta cells, which is similar to the effects of JAK inhibitors on spontaneous diabetes.⁴⁰ Remarkably, 2 weeks of treatment with JAK1/JAK2 inhibitor resulted in prolonged inhibition of islet immune infiltration and MHC class I upregulation, even after stopping treatment. We hypothesise that this may be because of the effects of JAK inhibition on memory T cells that are highly dependent on cytokines for survival.

Loss-of-function mutations in JAK1 or JAK2 in melanoma patients lead to resistance to checkpoint inhibitor therapies.^{42,43} Similarly, co-administration of the JAK inhibitor ruxolitinib and anti-PD-L1 also partially blocked the antitumour activity induced by anti-PD-L1.⁴⁴ These studies highlight the clinical importance of the JAK–STAT pathway in checkpoint inhibitor-mediated antitumour immune responses. We found that JAK inhibitor intervention before checkpoint inhibitors abrogated the antitumour response, but there was no effect on antitumour immunity when intervention was given after checkpoint inhibitor therapy. This demonstrates the JAK–STAT pathway is critical for initiating antitumour immune responses, and once established, the response is less vulnerable to inhibition by JAK inhibitors. IFN- γ signalling plays an important role in initiating antitumour immunity because it upregulates MHC expression on tumour cells and antigen-presenting cells,^{45,46} which is essential for subsequent T cell activation. JAK inhibitor treatment before checkpoint inhibitors could be preventing this initiation. Once tumour-specific T cells are activated, they can proliferate under

the control of γ c cytokines through multiple pathways, including the PI3K–Akt pathway, the RAS–MAPK pathway and the JAK–STAT pathway.^{47,48} When the JAK–STAT pathway is blocked after checkpoint inhibitor treatment, it is possible that the redundancy in these pathways helps preserve the antitumour T cell responses. We have only tested one model of tumour response to immune checkpoint blockade in this study, and clearly, more work needs to be done to confirm our results with other types of tumours.

An increasing number of studies indicate clinical characteristics that might be used as candidate predictors of checkpoint inhibitor-induced diabetes. Islet autoantibodies occur in half of checkpoint inhibitor-induced diabetes patients,^{14,49} and the T1D susceptibility allele HLA-DR4 is present in 60% of checkpoint inhibitor-induced diabetes patients.⁵⁰ These predictors may allow the identification of those who are at a higher risk of developing checkpoint inhibitor-induced diabetes and early intervention to halt beta cell destruction while minimising the effects on checkpoint inhibitor-induced antitumour immunity. Our study demonstrates the possibility of safe clinical use of JAK inhibitors in this scenario.

METHODS

Ethics statement

All experiments were conducted in accordance with the code of conduct of the National Health and Medical Research Council (NHMRC) of Australia and under the approval of the St Vincent's Hospital animal ethics committee (protocol 023/20) or the Harry Perkins Institute of Medical Research Animal Ethics Committee (protocol AE227).

Mice

NOD/Lt mice were bred and maintained at St. Vincent's Institute. All NOD mice used were females between 7 and 8 weeks of age. We used female NOD mice because of the sex bias for spontaneous diabetes in this strain. Female BALB/c.J mice were bred and maintained at the Harry Perkins Institute of Medical Research (Perth, WA, Australia) and were used between 8 and 10 weeks of age.

JAK1/JAK2 inhibitor

A suspension of the JAK1/JAK2 selective inhibitor LN3103801 (Eli Lilly) was prepared by sonicating the compound in

vehicle (0.5% methyl cellulose +0.25% Tween-80) for 90 min. Mice were treated with vehicle or LN3103801 (3 mg kg⁻¹) twice daily by oral gavage for 14 days.

Islet isolation

To isolate pancreatic islets, the bile duct was injected with 1.3 U mL⁻¹ collagenase P (Roche) in complete HBSS (Lonza Group), removed and digested for 17 min at 37°C in a water bath, followed by vigorous shaking for 1 min. The digested tissue was filtered through a 500-µm mesh and then washed with RPMI (Life Technologies Corp). Islets were purified using a histopaque-1077 density gradient (Sigma Aldrich) and dispersed into single cells using bovine trypsin (342 U mL⁻¹) and 2 mM EDTA in PBS. Finally, the cells were washed and rested in complete RPMI for at least 1 h at 37°C.

Preparation of single-cell suspensions

The peripheral lymphoid organs consisting of pooled spleen and non-draining lymph nodes (PLO) and pancreatic lymph nodes (PLN) were prepared by mechanical tissue disruption through a 70-µm cell strainer. The cell suspension was continued with 5 min red cell lysis and then washed with FACS buffer (0.5% FCS in PBS). After filtering through a nylon mesh, the single-cell suspension was ready for antibody staining.

Injection of BrdU

Bromo-deoxyuridine (BrdU) (Sigma Aldrich) powder was dissolved in warm PBS (10 mg mL⁻¹). Mice were injected i.p. with 200 µL (2 mg) of BrdU solution 16 h before harvesting.

Flow cytometry

Single-cell suspensions of islets were stained with PerCp-Cy5.5-labeled anti-CD45 antibody (30-F11) (BD Pharmingen) and biotinylated anti-H2-Kd (BD Pharmingen; SF1-1.1) followed by streptavidin-allophycocyanin (PE) (BioLegend) antibody. Islets, PLO and PLN cells were stained with the following antibodies from BD Pharmingen, BioLegend: anti-CD3-V500 (500 A2), anti-CD11c (N418), anti-B220 (RA3-6B2), anti-CD11b (M1/70), anti-F4/80 (BM8) conjugated to eFlour450 anti-CD4-FITC (GK1.5), anti-CD8-PE (Ly-2) or BV605 (53-6.7), anti-CD44-PE-cy7 (1M7), anti-CD62L-APC-cy7 (MEL-14) and anti-KLRG1-APC (MAFA). Dead cells were excluded using propidium iodide (PI, Calbiochem). Intracellular detection of BrdU was performed using the APC-BrdU FlowKit (BD Biosciences) after fixation, penetration and DNase process. Data were collected on the FACS Fortessa cell analyser (BD Bioscience) and were analysed using FlowJo Software version 10 (TreeStar, Inc).

Tetramer staining and magnetic bead-based enrichment

The tetramer staining and magnetic bead-based enrichment method were previously described.²⁵ Islet-specific

glucose-6-phosphatase catalytic subunit-related protein (IGRP)₂₀₆₋₂₁₄-specific CD8⁺ T cells were enriched by staining single-cell suspensions from PLO and PLN with Phycoerythrin (PE) conjugated (H2-Kd, VYLKTNVFL) tetramer (NIH Tetramer Core) on ice for 60 min. Cells were then washed and stained with anti-PE microbeads (Miltenyi Biotec). Magnetic separation was done using the AutoMACSpro (Miltenyi Biotec). The separated fractions were stained as described above and analysed by flow cytometry. For analysis, single cells were gated using forward and side scatter, live cells with propidium iodide negative staining. Then, the T cells were identified as CD3⁺dump⁻ (dump containing CD11c, CD11b, B220 and F4/80). IGRP-tetramer⁺CD44^{hi}CD8⁺ T cells were enumerated.

Immune checkpoint inhibitor therapy

To induce diabetes, 7–8-week NOD female mice were injected with three doses of 250 µg anti-PD-L1 monoclonal antibody (clone M1H5; Jip Biologics) intraperitoneally with a 2-day interval between each dose. Islets, PLN and PLO were harvested on day 9, or mice were monitored for diabetes development. For tumour therapy, 100 µg of anti-CTLA-4 (clone 9H10; Sigma Aldrich) was dosed once and anti-PD-L1 (Jip Biologics) was dosed 3 times with 2-day intervals at 100 µg as previously described.²⁶ Therapy was initiated when tumours were approximately 6–12 mm² in size.

Tumour cell lines

The murine mesothelioma cell line AB1-HA (Cell Bank Australia) was derived as previously described.²⁷ Cells were maintained in RPMI 1640 (ThermoFisher Scientific) supplemented with 20 mM HEPES, 0.05 mM 2-mercaptoethanol, 100 U mL⁻¹ penicillin (CSL Limited), 50 µg mL⁻¹ gentamicin (David Bull Labs), 10% Newborn Calf Serum (ThermoFisher Scientific) and 50 mg mL⁻¹ of geneticin (G418; Life Technologies Corp). All cell lines were tested for *Mycoplasma* spp., every 3 months by PCR and found to be negative. Cells were cultured for a minimum of four passages after thawing before inoculation into mice.

Tumour cell inoculation

Right-hand flanks of BALB/c mice were inoculated subcutaneously with 5 × 10⁵ tumour cells suspended in 100 µL of PBS. Mice were randomised for treatment when tumours were palpable. Tumour dimensions (length and width) were measured with digital callipers, and tumour growth was represented as area (mm²).

Analysis of diabetes

After anti-PD-L1 treatment, urine glucose levels were monitored daily in mice using Diastix (Bayer Diagnostics). Blood glucose levels were measured in mice with a positive glycosuria reading (> 110 mmol L⁻¹) using Advantage II Glucose Strips (Roche). Animals that displayed two consecutive blood glucose readings > 15 mmol L⁻¹ were

considered diabetic. For diabetes reversal, JAK1/JAK2 inhibitor or vehicle treatment was started on the day mice had a blood glucose level $> 15 \text{ mmol L}^{-1}$. Blood glucose levels were tested daily for 1 week and thrice weekly thereafter for 4 weeks. Mice with blood glucose $< 15 \text{ mmol L}^{-1}$ were considered cured.

Histology

Pancreases were fixed in Bouin's solution and paraffin-embedded, and 5- μm sections were cut from three levels (200 μm apart) and stained with haematoxylin and eosin (H&E). Insulinitis was scored using the following scale: islets scored as 0 (no infiltration), 1 (peri-islet infiltrate—leukocytes present at any point around the islet), 2 ($> 50\%$ peri-islet infiltrate), 3 (intraislet infiltrate) or 4 ($> 80\%$ intraislet infiltrate). The percentage of islets with each score per pancreas was calculated by the addition of the scores for the three sections. Between 36 and 156 islets/mouse were scored. Representative sections were photographed using an Olympus DP74 camera on a Leica DMRB microscope.

Statistical analysis

Statistical analysis was performed using GraphPad Prism 9 Software (GraphPad). All data are shown as bar graphs with individual mice, and the mean \pm SEM. $P < 0.05$ was considered significant. Flow cytometry data were analysed using unpaired *t*-tests or one-way ANOVA with post-tests for multiple comparisons where appropriate. Diabetes incidence curves were compared using the log-rank (Mantel-Cox) survival analysis. Tumour growth curves were compared using Mixed Model Type 3 Analysis of Variance (ANOVA), with Kenward–Roger Approximation using estimated marginal means for multiple comparisons of mean tumour sizes between all treatment groups for all time points.

ACKNOWLEDGMENTS

This work is supported by the National Health and Medical Research Council of Australia (NHMRC) Program grant (GNT1150425) and the Diabetes Australia Research Program. The St Vincent's Institute receives support from the Operational Infrastructure Support Scheme of the Government of Victoria. JC, AP and NP received support from the UWA Raine Foundation, Mesothelioma Applied Research Foundation and the US Department of Defence. JC and NP were funded by fellowships and scholarships from Cancer Council Western Australia and icare NSW Dust Diseases Board.

AUTHOR CONTRIBUTIONS

Tingting Ge: Conceptualization; data curation; formal analysis; investigation; methodology; writing – original draft; writing – review and editing. **Amber-lee Phung:** Formal analysis; writing – original draft. **Gaurang Jhala:** Formal analysis; methodology; writing – review and editing. **Prerak**

Trivedi: Formal analysis; methodology; writing – review and editing. **Nicola Principe:** Data curation; formal analysis; methodology; writing – review and editing. **David J De George:** Methodology; writing – review and editing. **Evan G Pappas:** Formal analysis; methodology. **Sara Litwak:** Formal analysis; methodology. **Laura Sanz-Villanueva:** Methodology; writing – review and editing. **Tara Catterall:** Methodology. **Stacey Fynch:** Methodology. **Louis Boon:** Resources. **Thomas Kay:** Funding acquisition; investigation; supervision; writing – review and editing. **Jonathan Chee:** Supervision; writing – review and editing. **Balasubramanian Krishnamurthy:** Supervision; writing – review and editing. **Helen E Thomas:** Conceptualization; funding acquisition; investigation; supervision; validation; writing – review and editing.

CONFLICT OF INTEREST

TWHK has an Investigator-Initiated Clinical Trial agreement with Eli Lilly. However, Eli Lilly had no role in the current study design, data collection and analysis, decision to publish or preparation of the manuscript. The authors declare that there are no other relationships or activities that might bias, or be perceived to bias, their work.

REFERENCES

- Paluch C, Santos AM, Anzilotti C, Cornall RJ, Davis SJ. Immune checkpoints as therapeutic targets in autoimmunity. *Front Immunol* 2018; **9**: 2306.
- Buchbinder EI, Desai A. CTLA-4 and PD-1 pathways: similarities, differences, and implications of their inhibition. *Am J Clin Oncol* 2016; **39**: 98–106.
- Waldman AD, Fritz JM, Lenardo MJ. A guide to cancer immunotherapy: from T cell basic science to clinical practice. *Nat Rev Immunol* 2020; **20**: 651–668.
- Pardoll DM. The blockade of immune checkpoints in cancer immunotherapy. *Nat Rev Cancer* 2012; **12**: 252–264.
- Baumeister SH, Freeman GJ, Dranoff G, Sharpe AH. Coinhibitory pathways in immunotherapy for cancer. *Annu Rev Immunol* 2016; **34**: 539–573.
- Ribas A. Tumor immunotherapy directed at PD-1. *N Engl J Med* 2012; **366**: 2517–2519.
- Sharpe AH, Pauken KE. The diverse functions of the PD1 inhibitory pathway. *Nat Rev Immunol* 2018; **18**: 153–167.
- Boutros C, Tarhini A, Routier E et al. Safety profiles of anti-CTLA-4 and anti-PD-1 antibodies alone and in combination. *Nat Rev Clin Oncol* 2016; **13**: 473–486.
- Postow MA. Managing immune checkpoint-blocking antibody side effects. *Am Soc Clin Oncol Educ Book* 2015: 76–83.
- Ferrari SM, Fallahi P, Elia G et al. Autoimmune endocrine dysfunctions associated with cancer immunotherapies. *Int J Mol Sci* 2019; **20**: 2560.
- Sznol M, Postow MA, Davies MJ et al. Endocrine-related adverse events associated with immune checkpoint blockade and expert insights on their management. *Cancer Treat Rev* 2017; **58**: 70–76.
- Akturk HK, Kahramangil D, Sarwal A, Hoffecker L, Murad MH, Michels AW. Immune checkpoint inhibitor-induced type 1 diabetes: a systematic review and meta-analysis. *Diabet Med* 2019; **36**: 1075–1081.

13. Barroso-Sousa R, Barry WT, Garrido-Castro AC et al. Incidence of endocrine dysfunction following the use of different immune checkpoint inhibitor regimens: a systematic review and meta-analysis. *JAMA Oncol* 2018; **4**: 173–182.
14. Stamatouli AM, Quandt Z, Perdigoto AL et al. Collateral damage: insulin-dependent diabetes induced with checkpoint inhibitors. *Diabetes* 2018; **67**: 1471–1480.
15. Wright JJ, Salem JE, Johnson DB et al. Increased reporting of immune checkpoint inhibitor-associated diabetes. *Diabetes Care* 2018; **41**: e150–e151.
16. Ansari MJ, Salama AD, Chitnis T et al. The programmed death-1 (PD-1) pathway regulates autoimmune diabetes in nonobese diabetic (NOD) mice. *J Exp Med* 2003; **198**: 63–69.
17. Hu H, Zakharov PN, Peterson OJ, Unanue ER. Cytocidal macrophages in symbiosis with CD4 and CD8 T cells cause acute diabetes following checkpoint blockade of PD-1 in NOD mice. *Proc Natl Acad Sci USA* 2020; **117**: 31319–31330.
18. Wang J, Yoshida T, Nakaki F, Hiai H, Okazaki T, Honjo T. Establishment of NOD-Pdcd1^{-/-} mice as an efficient animal model of type I diabetes. *Proc Natl Acad Sci USA* 2005; **102**: 11823–11828.
19. Lu J, Liu J, Li L, Lan Y, Liang Y. Cytokines in type 1 diabetes: mechanisms of action and immunotherapeutic targets. *Clin Transl Immunology* 2020; **9**: e1122.
20. Chong MM, Chen Y, Darwiche R et al. Suppressor of cytokine signaling-1 overexpression protects pancreatic beta cells from CD8⁺ T cell-mediated autoimmune destruction. *J Immunol* 2004; **172**: 5714–5721.
21. Kay TW, Campbell IL, Oxbrow L, Harrison LC. Overexpression of class I major histocompatibility complex accompanies insulinitis in the non-obese diabetic mouse and is prevented by anti-interferon- γ antibody. *Diabetologia* 1991; **34**: 779–785.
22. Thomas HE, Parker JL, Schreiber RD, Kay TW. IFN- γ action on pancreatic beta cells causes class I MHC upregulation but not diabetes. *J Clin Invest* 1998; **102**: 1249–1257.
23. Ge T, Jhala G, Fynch S et al. The JAK1 selective inhibitor ABT 317 blocks signaling through interferon- γ and common γ chain cytokine receptors to reverse autoimmune diabetes in NOD mice. *Front Immunol* 2020; **11**: 588543.
24. Trivedi PM, Graham KL, Scott NA et al. Repurposed JAK1/JAK2 inhibitor reverses established autoimmune insulinitis in NOD mice. *Diabetes* 2017; **66**: 1650–1660.
25. Chee J, Ko HJ, Skowera A et al. Effector-memory T cells develop in islets and report islet pathology in type 1 diabetes. *J Immunol* 2014; **192**: 572–580.
26. Zemek RM, De Jong E, Chin WL et al. Sensitization to immune checkpoint blockade through activation of a STAT1/NK axis in the tumor microenvironment. *Sci Transl Med* 2019; **11**: eaav7816.
27. Davis MR, Manning LS, Whitaker D, Garlepp MJ, Robinson BW. Establishment of a murine model of malignant mesothelioma. *Int J Cancer* 1992; **52**: 881–886.
28. Wong CP, Li L, Frelinger JA, Tisch R. Early autoimmune destruction of islet grafts is associated with a restricted repertoire of IGRP-specific CD8⁺ T cells in diabetic nonobese diabetic mice. *J Immunol* 2006; **176**: 1637–1644.
29. Clotman K, Janssens K, Specenier P, Weets I, De Block CEM. Programmed cell death-1 inhibitor-induced type 1 diabetes mellitus. *J Clin Endocrinol Metab* 2018; **103**: 3144–3154.
30. Harrison C, Kiladjian JJ, Al-Ali HK et al. JAK inhibition with ruxolitinib versus best available therapy for myelofibrosis. *N Engl J Med* 2012; **366**: 787–798.
31. Keystone EC, Taylor PC, Drescher E et al. Safety and efficacy of baricitinib at 24 weeks in patients with rheumatoid arthritis who have had an inadequate response to methotrexate. *Ann Rheum Dis* 2015; **74**: 333–340.
32. Winthrop KL, Cohen SB. Oral surveillance and JAK inhibitor safety: the theory of relativity. *Nat Rev Rheumatol* 2022; **18**: 301–304.
33. Smolen JS, Genovese MC, Takeuchi T et al. Safety profile of Baricitinib in patients with active rheumatoid arthritis with over 2 years median time in treatment. *J Rheumatol* 2019; **46**: 7–18.
34. Geginat J, Sallusto F, Lanzavecchia A. Cytokine-driven proliferation and differentiation of human naive, central memory, and effector memory CD4⁺ T cells. *J Exp Med* 2001; **194**: 1711–1719.
35. Rochman Y, Spolski R, Leonard WJ. New insights into the regulation of T cells by γ_c family cytokines. *Nat Rev Immunol* 2009; **9**: 480–490.
36. Zeng R, Spolski R, Finkelstein SE et al. Synergy of IL-21 and IL-15 in regulating CD8⁺ T cell expansion and function. *J Exp Med* 2005; **201**: 139–148.
37. Lin CL, Huang HM, Hsieh CL, Fan CK, Lee YL. Jagged1-expressing adenovirus-infected dendritic cells induce expansion of Foxp3⁺ regulatory T cells and alleviate T helper type 2-mediated allergic asthma in mice. *Immunology* 2019; **156**: 199–212.
38. Baecher-Allan C, Brown JA, Freeman GJ, Hafler DA. CD4⁺CD25^{high} regulatory cells in human peripheral blood. *J Immunol* 2001; **167**: 1245–1253.
39. Suri-Payer E, Amar AZ, Thornton AM, Shevach EM. CD4⁺CD25⁺ T cells inhibit both the induction and effector function of autoreactive T cells and represent a unique lineage of immunoregulatory cells. *J Immunol* 1998; **160**: 1212–1218.
40. Hamilton-Williams EE, Palmer SE, Charlton B, Slatery RM. Beta cell MHC class I is a late requirement for diabetes. *Proc Natl Acad Sci USA* 2003; **100**: 6688–6693.
41. Richardson SJ, Rodriguez-Calvo T, Gerling IC et al. Islet cell hyperexpression of HLA class I antigens: a defining feature in type 1 diabetes. *Diabetologia* 2016; **59**: 2448–2458.
42. Shin DS, Zaretsky JM, Escuin-Ordinas H et al. Primary resistance to PD-1 blockade mediated by JAK1/2 mutations. *Cancer Discov* 2017; **7**: 188–201.
43. Zaretsky JM, Garcia-Diaz A, Shin DS et al. Mutations associated with acquired resistance to PD-1 blockade in melanoma. *N Engl J Med* 2016; **375**: 819–829.
44. Luo N, Formisano L, Gonzalez-Ericsson PI et al. Melanoma response to anti-PD-L1 immunotherapy requires JAK1 signaling, but not JAK2. *Onco Targets Ther* 2018; **7**: e1438106.

45. Propper DJ, Chao D, Braybrooke JP *et al.* Low-dose IFN- γ induces tumor MHC expression in metastatic malignant melanoma. *Clin Cancer Res* 2003; **9**: 84–92.
46. Zhou F. Molecular mechanisms of IFN- γ to up-regulate MHC class I antigen processing and presentation. *Int Rev Immunol* 2009; **28**: 239–260.
47. Setrerrahmane S, Xu H. Tumor-related interleukins: old validated targets for new anti-cancer drug development. *Mol Cancer* 2017; **16**: 153.
48. Shourian M, Beltra JC, Bourdin B, Decaluwe H. Common γ chain cytokines and CD8 T cells in cancer. *Semin Immunol* 2019; **42**: 101307.
49. Hughes J, Vudattu N, Sznol M *et al.* Precipitation of autoimmune diabetes with anti-PD-1 immunotherapy. *Diabetes Care* 2015; **38**: e55–e57.
50. de Filette JMK, Pen JJ, Decoster L *et al.* Immune checkpoint inhibitors and type 1 diabetes mellitus: a

case report and systematic review. *Eur J Endocrinol* 2019; **181**: 363–374.

Supporting Information

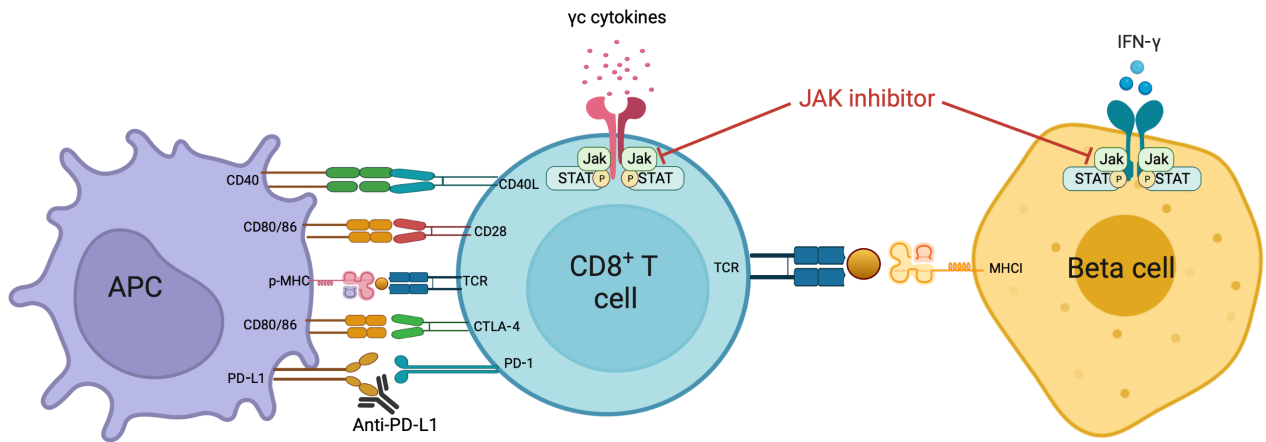
Additional supporting information may be found online in the Supporting Information section at the end of the article.



This is an open access article under the terms of the [Creative Commons Attribution-NonCommercial-NoDerivs](#) License, which permits use and distribution in any medium, provided the original work is properly cited, the use is non-commercial and no modifications or adaptations are made.

Graphical Abstract

The contents of this page will be used as part of the graphical abstract of html only. It will not be published as part of main.



Type 1 diabetes is a side effect of immune checkpoint inhibitor therapy for cancer. Here, we show that a JAK1/JAK2 inhibitor can prevent and reverse anti-PD-L1-induced diabetes in NOD mice by blocking common gamma chain cytokine activities in T cells and interferon-gamma function on beta cells. This study provides preclinical validation of the use of JAK inhibitors in checkpoint inhibitor-induced diabetes.